

# Selection of Gas Turbine Air Bottoming Cycle for Polish compressor stations

Daniel Czaja\*, Tadeusz Chmielniak, Sebastian Lepszy

*Institute of Power Engineering and Turbomachinery, Silesian University of Technology  
Konarskiego 18, Gliwice 44-100, Poland*

## Abstract

Gas turbines are one of the basic technologies used to produce electricity and power working machinery. The popularity of the technology results from its advantages, the most important of which are: fast start-up, high efficiency, low pollutant emissions, short construction time and reasonable size. Gas turbines are becoming increasingly important in new power installations.

Combined cycles can be used to increase the efficiency of energy systems. Examples of high efficiency cycles are combined cycle power plants (CCPP) and gas turbine air bottoming cycles (GT-ABC), which are a combination of a gas turbine and air turbine cycle coupled by means of a heat exchanger referred to as the Air Heat Exchanger (AHX). The main feature of the GT (and the GT-ABC) is low water consumption. For this reason, it can be used in gas transport and storage systems. The construction of this type of systems may turn out to be energy-effective due to the advancement in flow machinery construction, especially in the field of improvement to blade profiles and sealing.

This paper presents an application of gas-air systems with example configurations. Three technological structures are taken into consideration – a simple system ABC, an ABC with one air intercooler, and an advanced cycle with two intercoolers. To improve the efficiency of air turbine installations, more complex system configurations are required.

**Keywords:** Air Bottoming Cycle, Gas Turbine Air Bottoming Cycle, Air Heat Exchanger, Gas turbine, Air turbine, Intercooler

## 1. Introduction

In a conventional combined cycle power plant (CCPP) the exhaust heat of the gas turbine (GT) is utilized by the heat recovery steam generator (HRSG). In addition to the boiler and steam turbine

(ST), the cycle incorporates a condenser, pumps, piping, heat exchangers and many other devices, resulting in considerable costs. Importantly, even an advanced steam bottoming cycle (SBC) provides only one third of total plant power. Another disadvantage of the SBC is the long start-up period. The use of an air bottoming cycle (ABC) offers a significant increase in power and efficiency without the complexity of the SBC. ABC, which requires no water (no steam), looks attractive for power generation in small units (under 50 MW range) [1] and in compressor

\*Corresponding author

*Email addresses:* daniel.czaja@polsl.pl (Daniel Czaja\*), tadeusz.chmielniak@polsl.pl (Tadeusz Chmielniak), sebastian.lepszy@polsl.pl (Sebastian Lepszy)

stations. According to [2] there are two main objectives of ABC:

- to provide a combined thermodynamic cycle system that is coupled to a gas turbine and which has a greater thermodynamic efficiency than the GT alone,
- to retain the operational flexibility and reliability of the GT,

The ABC thermal engine involves a multi-stage compression process where air passes through stages of compression and cooling. Prior to expanding in the turbines, the air passes through an air heat exchanger (AHX). An important component in terms of the efficiency of the entire configuration of the gas turbine with ABC is the AHX coupling the two systems. The most important parameters impacting the optimum selection of the AHX are pressure drops and temperature differences. High efficiencies of the cycle are achieved for small temperature differences in the AHX, which result in its large dimensions. Other possible structural solutions are: shell-and-tube or plate heat exchangers. For modeling purposes, plate heat exchanger (PHE) was applied.

In the case of a gas turbine unit, the hot gases are expanded in a turbine to produce torque, which is used to drive an air compressor. The remaining torque is available on an output shaft [3]. This can be used, for example, to drive a natural gas compressor in a gas station. The option of GT with steam reforming for exhaust heat recovery in a remote compressor station applications was discussed by [4]. Configuration of GT with ABC was also analyzed by [5–7]. Performance analyzes of gas turbine air – bottoming combined system and industry applications analysis were carried out by [8–10]. Thermodynamic analysis of ABC as well as the results of a feasibility study for using ABC for gas turbines waste heat recovery/power generation on oil/gas platforms in the North Sea are to be found in [11].

Research on gas-air systems was done by [12]; it focused on applications in heat engineering and systems used to power working machinery in the gas transport and storage industry [13]. The use of gas-air systems as a heat source for the CCS installation of a coal-fired power unit was also done by [14].

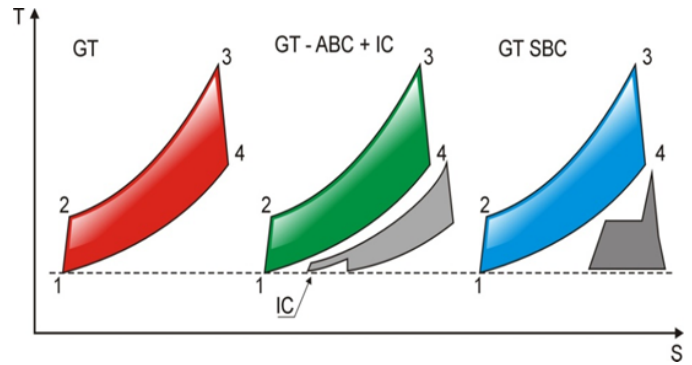


Figure 1: Comparison between individual gas turbine systems

Thermodynamic analysis of ABC as well as exergy analysis of GT-ABC was conducted by [15–17].

Gas-air systems can find application:

- in the food sector (industrial bakeries, powdered milk factories),
- as a source of hot air in furnaces for glass melting,
- in high-temperature furnace systems where pre-heated air comes from ABC,
- in offshore locations; gas-air systems can be used to improve the efficiency of simple power units with gas turbines operating at locations without access to large amounts of fresh water.

The mechanical power obtained from the turbine can be used either to support the gas turbine system or to generate electricity. Owing to the short start-up time of the air turbine, the ability to meet peak demand for power may also be significant. Air turbine systems are simple in terms of operation. This is due to the absence of: (i) a combustion process, (ii) toxic media or (iii) media causing erosion or needing to be topped up. ABC also improves the performance of the new combined engine in off-design mode [2]. It is expected that ABC will require much lower investment expenditure in respect of CCPP [18].

Fig. 1 shows a comparison in a T-s diagram between: recuperated gas turbine, gas turbine air bottoming cycle (GT-ABC) – also known as dual gas turbine – and gas turbine steam bottoming cycle (GT-SBC).

Table 1: Włocławek compressor station basic data [19, 20]

Parameter	Value
Gas composition	96.3% CH <sub>4</sub> , 2.89% C <sub>2</sub> H <sub>6</sub>
Gas inlet pressure (to compressor station)	approx. 6.05 MPa
Gas outlet pressure (from compressor station)	approx. 8.35 MPa
Volume flow	7,694,000 Nm <sup>3</sup> /h
Gas inlet temperature (average annual)	9°C
Gas outlet temperature	<30°C

Table 2: GT10 gas turbine basic data [19, 20]

Parameter	Value
Shaft power	25 MW
Efficiency (nominal point)	35.2%
Revolutions	7700 rpm
Max. revs of turbine	8625 rpm

The main goal of this paper is to determine the basic thermodynamic characteristics of the systems under analysis. Increases in mechanical power output and energy efficiency are determined. Improvement of the GT engine can be interesting from the point of view of obtaining additional power.

## 2. Compressor station description

There are five gas compressor stations in the Polish section of the “Yamal Western Europe” gas pipeline. They are tasked with providing sufficient pressure to compensate for flow friction losses. Each compressor aggregate has 25 MW of power and consists of a centrifugal compressor and gas turbine

Table 3: 50P2 compressor basic data [18, 19]

Parameter	Value
Suction pressure	6.4 MPa
Discharge pressure	8.45 MPa
Revolutions	6680 rpm
Flow	c. 2 million Nm <sup>3</sup> /h

unit. Compressor aggregates are grouped in parallel. They also contain the gas coolers and their own compressor and turbine control system. Every unit can be controlled from the Distributed Control System (DCS). Nominal discharge pressure is 8.45 MPa. Yearly, 40 billion Nm<sup>3</sup> of gas can be compressed [19]. The basic data of an example compressor station are shown in Table 1. Technical data of the GT10 gas turbine and 50P2 compressor are presented in Tables 2–3 [19, 20]. Nm<sup>3</sup> refers to gas volume at normal temperature and pressure, which are 0°C and 101.325 kPa.

This section of the 4,107 km-long Yamal – Europe pipeline includes five compressor stations at Ciechanow, Szamotuly, Zambrow, Włocławek and Kondratki. The stations have a total driving power of 600 MW and feature four to six turbocompressor units driven by a 25 MW gas turbine.

## 3. Technological structures under analysis

ABC is a Brayton cycle that utilizes the exhaust heat from a topping GT engine. The configuration where the ABC cycle recuperates heat from topping GT cycles is also referred to as a dual gas turbine combined cycle [21].

In a simple gas-air system a compressor with no intercooler (Case A), a heat exchanger AHX coupling the gas and air systems, and an air turbine are used. Referring to Fig. 2 a gas turbine includes a compressor and combustion chamber. The products of combustion and excess air are applied to a turbine where they power an output shaft (and drive a compressor). After expansion, gases exit the turbine at high temperature. The exhaust gas duct conveys them to an air heat exchanger where they give up a substantial portion of their energy to heat up compressed air. The next step is to expand the air in the air turbine and produce torque.

To improve the efficiency of air turbine installations, it is necessary to employ more complex system configurations. An example of a complex air turbine system is the installation shown in Fig. 3 (Case B). A first compressor stage compresses ambient air. Then compressed air is conveyed to an intercooler (IC) and cooled to the lowest possible temperature. After intercooling the compressed air

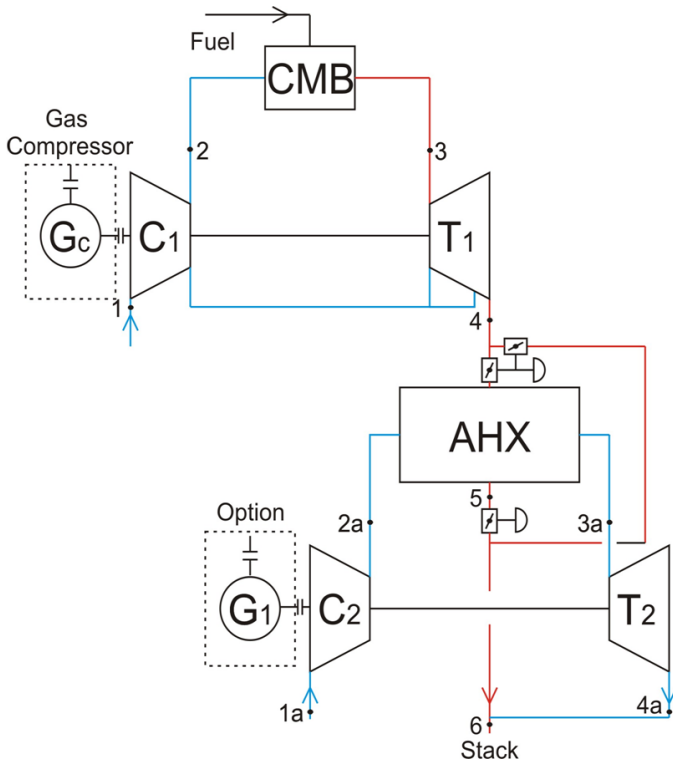


Figure 2: Simple gas-air system (Case A)

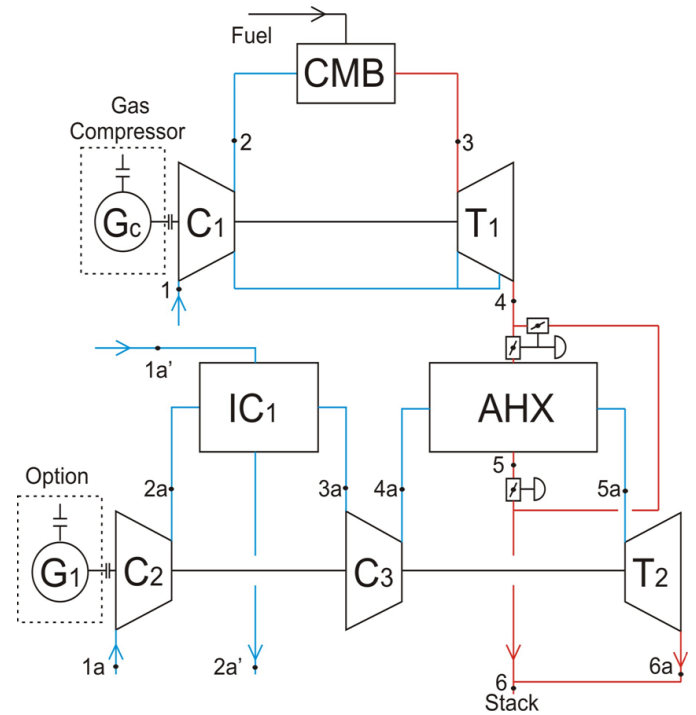


Figure 3: Complex gas-air system with an air intercooler (Case B)

is again compressed in a second air compressor and then air is heated up in AHX. Afterwards the air is expanded in the air turbine as in Case A. The compression process is nearly adiabatic. The intercooler is used between an adjacent pair of compressors to keep the temperature of the compressed air low before compression and make the work of compression more efficient. The compressed air is passed through AHX where its temperature is raised by the hot GT's exhaust gas flowing in the AHX counterflow. Afterwards the hot compressed air is expanded in the air turbine and torque is produced. Intercooling between the compressors helps to increase the heat transfer in the recuperator by reducing the overall compressor discharge temperature. The compressor work is also reduced, while the available work from the turbine is increased.

The most complex installation considered is presented in Fig. 4 (Case C). The outlet air from compressor C3 (system with one intercooler) and C4 is at lower temperatures than the simple system, which allows for a more intense cooling of the gas turbine flue gases and a reduction in the driving operation of the compressors. It should be noted that the in-

tercoolers here are air cooled heat exchangers. The compressor work is also reduced, while the available work from the turbine is increased.

#### 4. Calculations

The target of a GT-ABC system analysis should be to maximize the ratio of generated electricity to the chemical energy of the fuel. In this case, the energy efficiency of the system can be defined as follows:

$$\eta_{elGT-ABC} = \frac{N_{elGT} + N_{elAT}}{\dot{m}_f \cdot LHV} \quad (1)$$

ABC system efficiency can be evaluated using the following definition of energy efficiency:

$$\eta_{eAT} = \frac{N_{mAT}}{\dot{Q}_4} \quad (2)$$

where:  $\dot{Q}_4$  is the heat of cooling flue gases to the reference temperature.

In order to simplify the analyses, it is assumed in the calculations presented in this paper that  $\dot{Q}_4$  corresponds to the cooling of flue gases to temperature  $t_5 = 15^\circ\text{C}$ , while the water vapor contained in flue gases is not condensed.

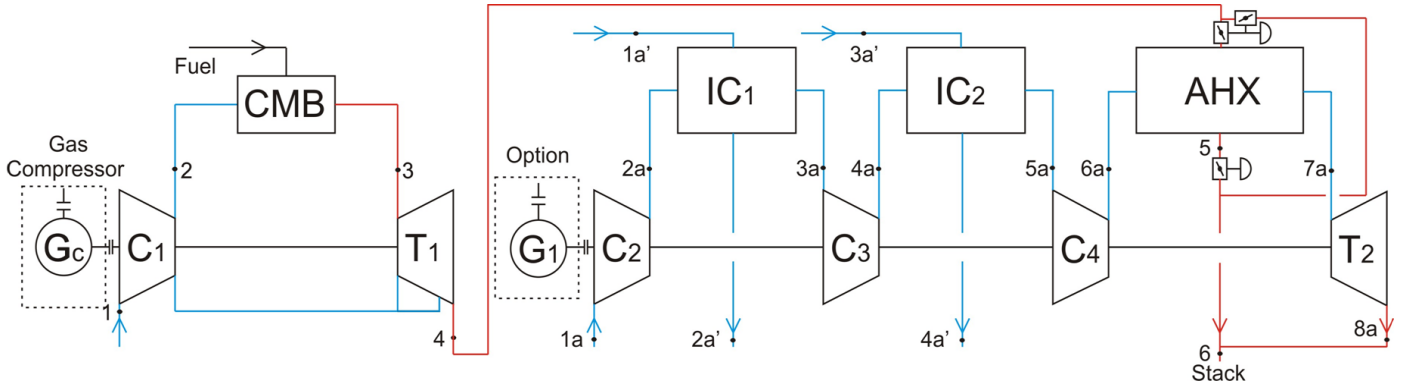


Figure 4: Complex gas-air system with two air intercoolers (Case C)

By adopting some simplifying assumptions, it is possible to determine the dependence between the energy efficiency of the gas turbine and air turbine systems, as well as of the entire system. The most important simplifying assumption is that there are no radiation heat losses from either the gas or the air turbine. The dependence can be defined as follows:

$$\eta_e = \eta_{eGT} + \eta_{eAT} (1 - \eta_{eGT}) \quad (3)$$

Calculations of system parameters were performed using the authors' own algorithms (ideal gas model; heat capacity as a function of gas temperature).

The GT-ABC system is optimized in terms of energy efficiency. The pressure ratio and the air mass flow are chosen as decision variables. The other values are selected according to the parameters of the machines and equipment operating in gas turbine systems. In Case A for set parameters of the heat exchanger (AHX effectiveness), pressure value  $p_{2a}$  is varied within the determined range. The procedure is repeated for different mass flow values of the air sucked in by compressor  $C_2$ .

In complex systems it is important to choose an appropriate pressure value at the outlet of each stage of the compressor. For example, in the case C the optimum pressure value which minimizes the power consumption used to drive the compressor can be determined by minimizing the following objective function [22].

$$[T_{1a} (\zeta_1 - 1) + T_{3a} (\zeta_3 - 1) + T_{5a} (\zeta_5 - 1)] \frac{1}{\eta_i} \rightarrow \min \quad (4)$$

$$\text{where: } \zeta_1 = \frac{T_{2as}}{T_{1a}}, \zeta_3 = \frac{T_{4as}}{T_{3a}}, \zeta_5 = \frac{T_{6as}}{T_{5a}}$$

The procedure is repeated for different values of the air mass flow sucked by the first stage compressor. The result where energy efficiency reaches the highest value is taken as the optimized structure.

The pressure drops in the heat exchanger are the parameters which have a significant impact on the efficiency of the entire system. The higher the pressure drop in AHX, the lower the efficiency  $\eta_{eAT}$ . On the other hand, a bigger pressure drop makes it possible to obtain high heat transfer coefficients, which leads to a reduction in the heat exchange area and, consequently, to a smaller sized device. A plate heat exchanger (PHE) was applied for modeling purposes. PHE are widely employed in chemical, food and pharmaceutical process industries. They are compact, easy to clean, efficient and very flexible [23]. In order to determine the heat transfer coefficient many physical properties of air and exhaust gas were taken into account:

$$\alpha = f(m, \lambda, c_p, \rho, \nu, \Delta t, a \dots) \quad (5)$$

The calculation algorithm is based on the LMTD method [24]. To determine the heat surface area the Nusselt number should be found. The Nusselt number for this type of heat exchangers can be defined by the formula [25]:

$$Nu = 0.022 \cdot \sqrt{\xi_0} \cdot \beta \cdot \beta_t \cdot Re^{0.825} \cdot Pr^{0.54} \quad (6)$$

where:  $\xi_0$  – flow resistance ratio,  $\beta$  – turbulence damping ratio,  $\beta_t$  – forced turbulence ratio.

It is assumed that the wall which separates media in the heat exchanger is made of P235GH and 16Mo3

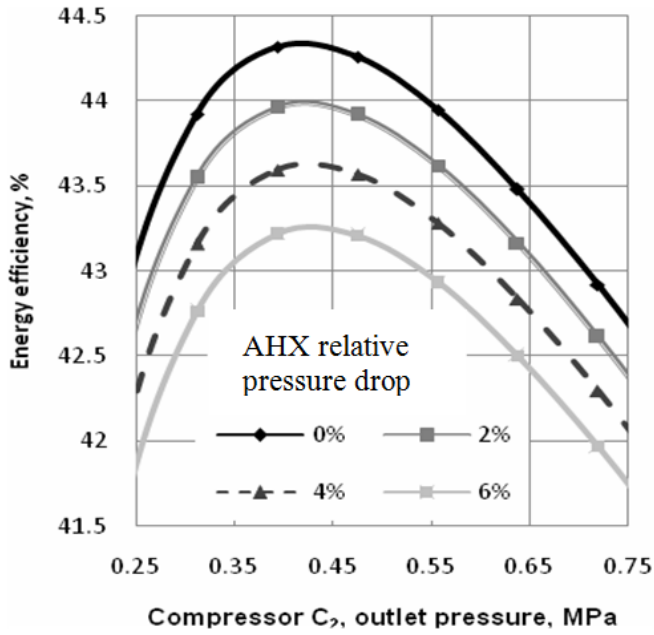


Figure 5: Energy efficiency as a function of pressure ratio (Case A)

steel, and its heat conductivity depends on temperature. Also 13CrMo4-5 is taken into account for surfaces which work in high temperature areas.

Depending on minimal product  $m \cdot c_p$  of considered fluids, the effectiveness of AHX and IC can be defined as follows:

$$\varepsilon = \frac{T_{inhot} - T_{outhot}}{T_{inhot} - T_{incold}} \quad (7)$$

$$\text{if } (m \cdot c_p)_{min} = (m \cdot c_p)_{cold},$$

$$\varepsilon = \frac{T_{outcold} - T_{incold}}{T_{inhot} - T_{incold}} \quad (8)$$

$$\text{if } (m \cdot c_p)_{min} = (m \cdot c_p)_{hot}$$

## 5. Results and discussion

The results of energy efficiency and increase in mechanical power output for different pressure drops in the AHX are presented in Fig. 5 and Fig. 6 (Case A). The value of pressure drop always refers to the inlet pressure of individual heat exchangers. Presented results are obtained for polytropic efficiency of turbomachinery  $\eta_{pC2} = \eta_{pT2} = 88\%$  and effectiveness of AHX  $\epsilon_{AHX} = 96\%$ . The optimal air mass flow is equal  $\dot{m}_a = 80.46$  kg/s. For a pressure ratio

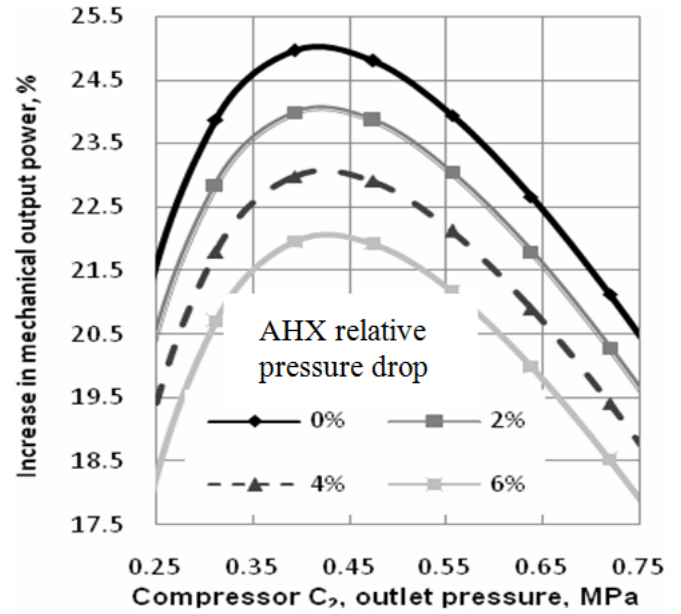


Figure 6: Mechanical power output as a function of pressure ratio (Case A)

$\beta_{C2} = P_2/P_1 = 3.88$  ( $\Delta P_{AHX} = 0\%$ ) the highest energy efficiencies and the maximum value of mechanical power output are recorded. Efficiency is linearly dependent on mechanical power output. Therefore, the maximum increase in mechanical power output and energy efficiency is for the same pressure ratio. The exhaust gas temperature from ABB GT10 value is equal  $T_4 = 813$  K. A drop in the exhaust gas temperature results in a considerable decrease in energy efficiency.

Increase in mechanical power output was determined according to formula 9.

$$\Delta N = \frac{N_{ABC}}{N_{GT}} \cdot 100\% \quad (9)$$

More significant increases in efficiency compared to Case A are achieved only for high values of polytropic efficiency of turbo machines. Presented results for Case B (Fig. 7–8) are obtained for polytropic efficiency of turbomachinery  $\eta_{pCi} = \eta_{pT2} = 88\%$  and effectiveness of AHX  $\epsilon_{AHX} = 96\%$ ,  $\epsilon_{IC} = 90\%$ . The optimal air mass flow is almost the same like in case A ( $\dot{m}_a = 80.56$  kg/s). The pressure ratio of compressor  $C_2$  is  $\beta_{C2} = P_2/P_1 = 2.41$  and outlet pressure of compressor  $C_3$  varied within the determined range.

The energy efficiency obtained for various pres-

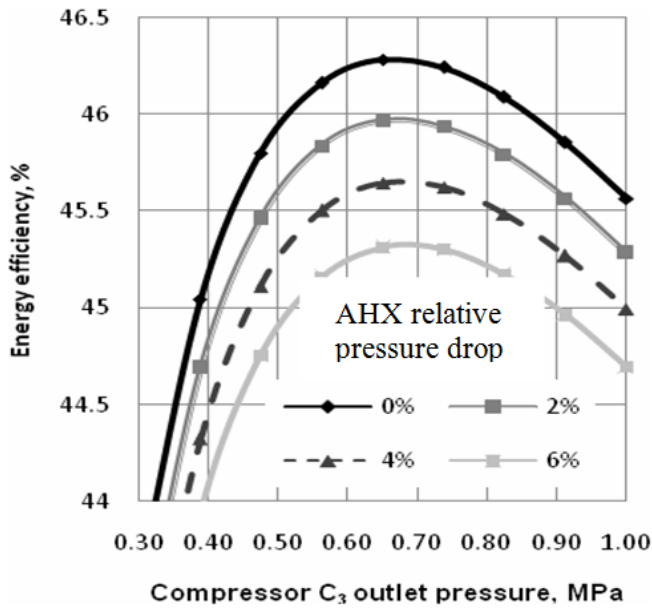


Figure 7: Energy efficiency of a complex system as a function of pressure ratio (Case B)

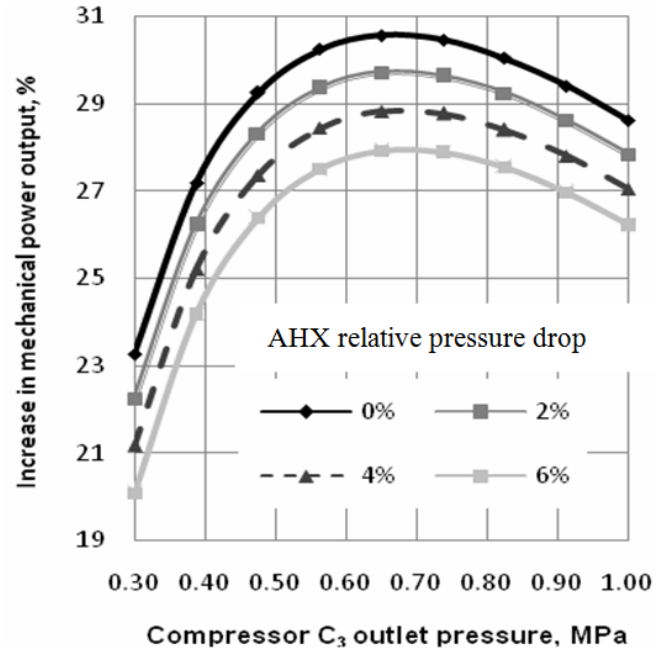


Figure 8: Mechanical power output of a complex system as a function of pressure ratio (Case B)

sure ratios was dependent on the technical structure. The cycle with two intercoolers had the highest pressure ratio (Fig. 9–10). This system also has high energy efficiency across a wide range of pressure ratios. The pressure drop in heat exchangers shows a similar trend. The calculation made for polytropic efficiency was  $\eta_{pCi} = \eta_{pT} = 0.88$  and for effectiveness of AHX  $\epsilon_{AHX} = 0.96$  ( $\epsilon_{ICi} = 0.9$  respectively).

Energy efficiency as a function of compressor ratio for each of analyzed cases is shown in Fig. 11. The curves illustrate two different levels of pressure drop. The system with two intercoolers enjoys high energy efficiency across a wide range of pressure ratios. On the other hand there is a very significant increase in energy efficiency between GT-ABC with no inter-stage cooler and GT-ABC with one IC.

The dependence between AHX and intercooler effectiveness and their influence on the energy efficiency of the cycle is presented in Fig. 8. Calculations were made parametrically for the purpose of comparing the energy efficiency value of the reference case ( $\eta_{pCi} = \eta_{pT2} = 88\%$ ,  $\epsilon_{IC} = 90\%$ ,  $\epsilon_{AHX} = 96\%$ ,  $\eta_{eGT-ABC} = 46.28\%$ ).

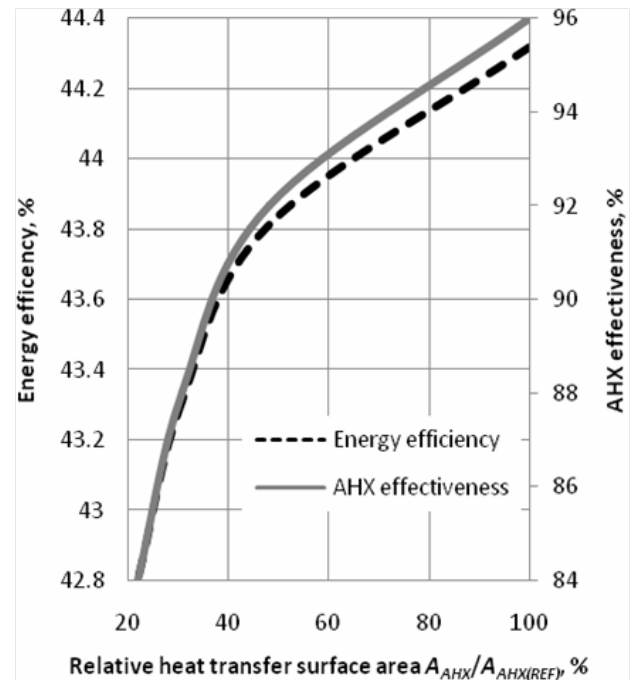


Figure 13: The impact of relative heat transfer surface area on energy efficiency and AHX effectiveness

The heat exchanger AHX is characterized by a large heat transfer surface area to achieve high heat exchanger effectiveness. The influence of heat transfer surface area on effectiveness and energy effi-

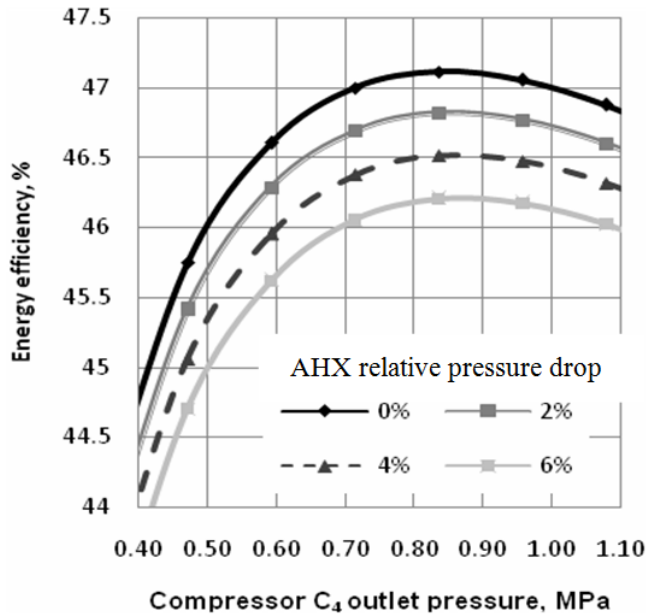


Figure 9: Energy efficiency of a complex system as a function of pressure ratio (Case C)

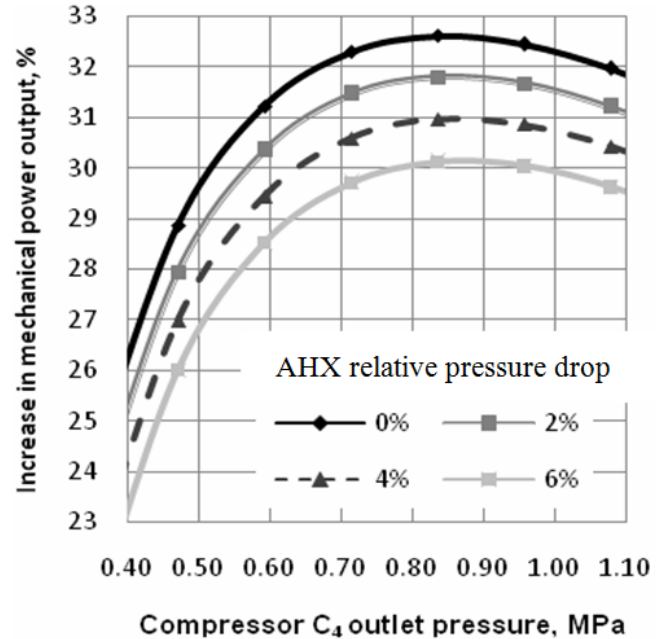


Figure 10: Mechanical power output of a complex system as a function of pressure ratio (Case C)

ciency was considered and the results are shown in Fig. 12. The value 100% of relative heat transfer surface area represents a heat transfer surface area equal to about  $A_{AHX(REF)} = 89,000 \text{ m}^2$  (for  $\epsilon_{AHX} = 96\%$ ). The curves illustrate polytropic efficiency of turbomachinery  $\eta_{pC2} = \eta_{pT2} = 88\%$ . Increasing the heat transfer surface area results in a much larger AHX, but also higher energy efficiency of the system. The impact of relative heat transfer surface area on energy efficiency and AHX effectiveness is presented in Fig. 13 (results for Case A).

A comparison of Case A and Case B is presented in Table 4. Calculations were made for polytropic efficiency of turbomachinery  $\eta_{pCi} = \eta_{pT2} = 88\%$ , effectiveness of intercooler  $\epsilon_{IC} = 75\%$ , effectiveness of AHX  $\epsilon_{AHX} = 88\%$  and the same pressure drop value on the both sides of heat exchangers equal  $\Delta P_{AHX} = \Delta P_{IC} = 4\%$ . Optimal mass flow, pressure ratio, increase in mechanical power output and heat transfer surface area were determined.

## 6. Conclusion

The analyzes presented in this paper show that the considered gas turbine systems coupled with an air system (GT ABC) is very interesting from the point of view of power engineering. Their energy efficiency is higher than that of stand-alone gas turbine units. The systems are characterized by high values of overall efficiency. The most efficient considered installation of Case A can reach  $\eta_{eGT-ABC} = 44.31\%$  when  $\eta_{pC2} = \eta_{pT2} = 88\%$ ,  $\epsilon_{AHX} = 96\%$  and pressure drop in AHX is omitted. The increase in mechanical power output is  $\Delta N = 24.95\%$  for this case. Using an additional facility such as an intercooler (Case B), electricity generation efficiency rose to  $\eta_{eGT-ABC} = 46.28\%$  ( $\Delta N = 30.56\%$ ,  $\eta_{pCi} =$

Table 4: Comparison between Cases A, B and C

Parameter	Case A	Case B	Case C
$\Delta P_{AHX} = \Delta P_{IC}, \%$	4	4	4
$\eta_{eGT-ABC}, \%$	42.61	43.71	44.03
$\Delta N, \%$	20.28	23.51	24.17
$\beta_{C2}, -$	3.88	2.12	1.92
$\beta_{C3}, -$	N/A	2.78	2.04
$\beta_{C4}, -$	N/A	N/A	2.37
$A_{AHX}, \text{m}^2$	$\sim 27,500$	$\sim 27,000$	$\sim 26,500$
$A_{IC1}, \text{m}^2$	N/A	$\sim 10,600$	$\sim 10,600$
$A_{IC2}, \text{m}^2$	N/A	N/A	$\sim 10,600$
$m_a, \text{kg/s}$	80.92	81.06	81.08

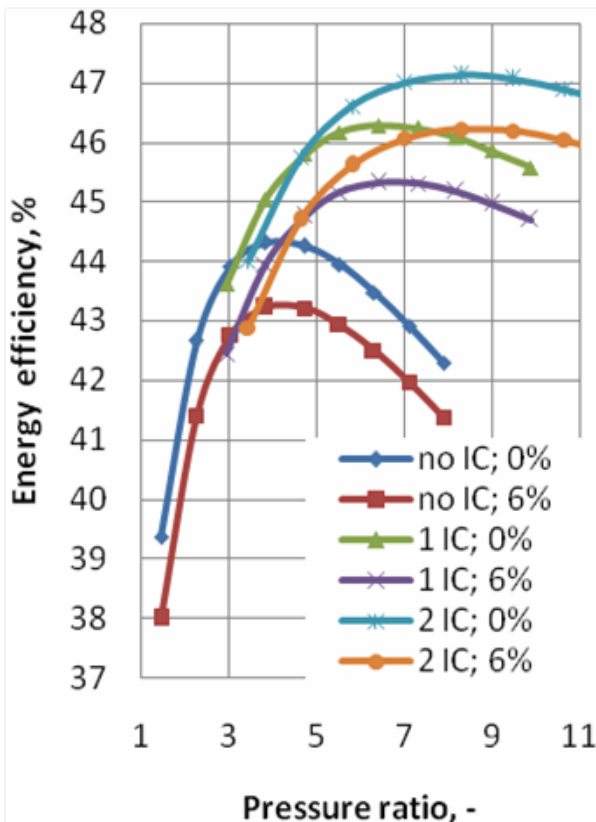


Figure 11: Energy efficiency of analyzed cases

$\eta_{pT2} = 88\%$ ,  $\epsilon_{AHX} = 96\%$ ,  $\epsilon_{IC} = 90\%$  and pressure drop is omitted). The most significant increase in energy efficiency and mechanical power output is assigned to Case C, where two intercoolers were adopted  $\eta_{eGT-ABC} = 47.12\%$  ( $\Delta N = 32.63\%$ ,  $\eta_{pCi} = \eta_{pT2} = 88\%$ ,  $\epsilon_{AHX} = 96\%$ ,  $\epsilon_{IC} = 90\%$  and pressure drop is omitted). The use of this type of installation may take place if the economic analysis is strongly affected by the main advantages of GT-ABC systems, such as the low water consumption, operation flexibility and the potential to meet peak demand for energy. The thermodynamic potential of GT-ABC was shown. The energy efficiency and increase in mechanical power output were determined. A competitive cycle in respect of SBC for power engineering where is a lack of water was presented.

Further investigations are required to show all advantages of the GT-ABC engine in relation to other cycles such as [26–28]. Improvement of existing engineering achieves higher values of energy efficiency and increases in mechanical power output on the shaft (shafts). Further investigation may bring

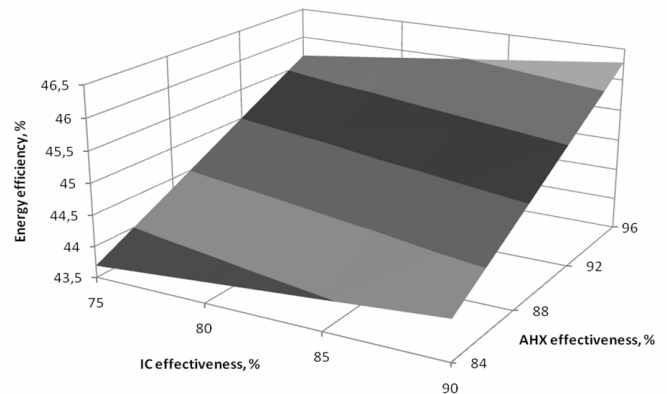


Figure 12: The influence of AHX and IC effectiveness on energy efficiency

to light additional improvements to the GT-ABC engine.

#### Acknowledgments

The results presented in this paper were obtained from research work co-financed by the National Centre of Research and Development in the framework of Contract SP/E/1/67484/10 – “Strategic Research Programme – Advanced Technologies for obtaining energy: Development of a technology for highly efficient zero-emission coal-fired Power units integrated with CO<sub>2</sub> capture”.

#### References

- [1] M. Korobitsyn, New and advanced energy conversion technologies. Analysis of cogeneration, combined and integrated cycles, Amsterdam, 1998.
- [2] L. Kambanis, Analysis and modeling of power transmitting systems for advanced marine vehicles, Massachusetts Institute of Technology, 1995.
- [3] W. Farrell (June 1998).
- [4] K. Botros, M. de Boer, H. Fletcher, Thermodynamics, environmental and economic assessment of crgt for heat recovery in remote compressor station applications, in: ASME Paper, no. 97-GT-510, 1997.
- [5] Anonymous, Low cost “air bottoming cycle” for gas turbines, in: Gas Turbine World, 1991.
- [6] K. Weston, Dual gas turbine combined cycles, in: Proceedings of the 28th Intersociety Energy Conversion Engineering Conference EIECEC’93, Boston, 1993, pp. 955–958.
- [7] F. Wicks, C. Wagner, Synthesis and evaluation of a combined cycle with no steam nor cooling water requirements, in: Proceedings of the 28th Intersociety Energy Conversion Engineering Conference EIECEC’93, Boston, 1993, pp. 105–110.

- [8] M. Korobitsyn, Industrial applications of the air bottoming cycle, *Energy Conversion and Management* 43 (2002) 1311–1322.
- [9] S. Yousef, H. Najjar, M. S. Zaamout, Performance analysis of gas turbine air-bottoming combined system, *Energy Conversion and Management* 37 (4) (1996) 399–403.
- [10] M. Ghazikhani, M. Passandideh-Fard, M. Mousavi, Two new high-performance cycles for gas turbine with air bottoming, *Energy* 36 (2011) 294–304.
- [11] O. Bolland, M. Forde, B. Hande, Air bottoming cycle: Use of gas turbine waste heat for power generation, *Journal of Engineering for Gas Turbines and Power* 118 (2) (1996) 359–368.
- [12] T. Chmielniak, D. Czaja, S. Lepszy, Wykorzystanie układów gazowo-powietrznych w ciepłownictwie, in: *Rynek Ciepła 2011*, Kaprint Lublin, 2011.
- [13] T. Chmielniak, S. Lepszy, D. Czaja, Analysis of gas turbine air-bottoming-cycle and heat exchanger modelling, in: *Proceedings of ECOS 2011*, Novi Sad, Serbia, 2011.
- [14] T. Chmielniak, S. Lepszy, D. Czaja, The use of air-bottoming cycle as a heat source for the carbon dioxide capture installation of a coal fired power unit, *Archives of Thermodynamic* 32 (3) (2011) 89–101.
- [15] J. Kaikko, L. Hunyadi, Air bottoming cycle for cogeneration of power, heat and cooling, Department of Energy Technology, Royal Institute of Technology, Sweden.
- [16] A. Tiwari, M. Islam, M. Khan, Thermodynamic analysis of combined cycle power plant, *International Journal of Engineering Science and Technology* 2 (4) (2012) 480–491.
- [17] M. Ghazikhani, H. Takdehghan, A. Moosavi Shayegh, Exergy analysis of gas turbine air bottoming combined cycle for different environment air temperature, in: *Proceedings of 3rd International Energy, Exergy and Environment Symposium*, 2007.
- [18] T. Chmielniak, D. Czaja, S. Lepszy, Technical and economic analysis of the gas turbine air bottoming cycle, in: *Proceedings of ASME Turbo Expo 2012*, 2012.
- [19] Transit gas pipeline system.  
URL [http://www.europolgaz.com.pl/gazociag/tlocznie\\_gazu](http://www.europolgaz.com.pl/gazociag/tlocznie_gazu)
- [20] ABB Zamech Gazpetro Sp. Z o. o. Information brochure.
- [21] K. Weston, Dual gas turbine combined cycles, in: *Proceedings of the 28th Intersociety Energy Conversion Engineering Conference IECEC'93*, Vol. 1, Boston, USA, 1993, pp. 955–958.
- [22] J. Szargut, *Termodynamika techniczna*, Wydawnictwo Politechniki Śląskiej, Gliwice, 2005.
- [23] J. Gut, J. Pinto, Modeling of plate heat exchangers with generalized configurations, *International Journal of Heat and Mass Transfer* 46 (2003) 2571–2585.
- [24] E. Kostowski, *Przepływ ciepła*, Wydawnictwo Politechniki Śląskiej, Gliwice, 2000.
- [25] L. Zander, Z. Zander, Projektowanie płytowych wymienników ciepła, *Instalacje Sanitarne* 2 (7) (2003) 27–30.
- [26] T. Chmielniak, S. Lepszy, Technical and economical analysis of gas-turbine systems with external combustion of the biomass, *Archives of thermodynamics* 28 (3) (2007) 67–80.
- [27] T. Chmielniak, S. Lepszy, External combustion of biomass parallelly coupled with the gas turbine unit, in: *SYMKOM'05 Compressor and turbine flow systems – theory and application areas*, Institute of Turbomachinery, Technical University of Łódź, Łódź, 2005.
- [28] M. Liszka, G. Manfrida, A. Ziębik, Parametric study of hrsg in case of repowered industrial chp plant, *Energy Conversion and Management* 44 (2003) 995–1012.

## Nomenclature

$\alpha$  Heat transfer coefficient, W/(m<sup>2</sup>K)

$\beta$  Pressure ratio, -

$\Delta$  Difference, increase, -

$\epsilon$  Effectiveness,

$\lambda$  Thermal conductivity, W/(m K)

$\rho$  Density, kg/m<sup>3</sup>

$\nu$  Kinematic viscosity, m<sup>2</sup>/s

$\zeta$  Temperature ratio, -

$\dot{m}$  Mass flow rate, kg/s

$c_p$  Specific heat, J/(kg K)

A Heat transfer surface area, m<sup>2</sup>

a Thermal diffusivity, m<sup>2</sup>/s

AT Air Turbine

CMB Combustion chamber

G Generator

LHV Lower heat value, J/kg

$\mu$  Dynamic viscosity, Pa·s

N Power, %

Nu Nusselt number, -

p,P Pressure, MPa

Pr Prandtl number, -

R Gas constant, J/(kg K)

Re Reynolds number, -

T, t Temperature, K, °C

1,1a,2... refers to individual reference points (Fig.2-4)

a Air

ABC Air Bottoming Cycle

AT Air turbine

C Compressor

c Cycle

cold Cold medium

e Energetic

el Electric

f Fuel

G Generator

GT Gas turbine

hot Hot medium

i Internal, isentropic

in Inlet

m Mechanical

out Outlet

p Polytropic

ref Reference case

T Turbine

t Temperature, K, °C